

Encapsulation study of citalopram and risperidone into nanostructured silica SBA-15 for in vitro release evaluation

Magali Naomi Tanaka¹ · Solange Teixeira Soares Santos² · Marize Gouveia³ · Mery dos Santos Filho⁴ · Ivana Conte Cosentino⁵ · Jair Borges Barbosa Neto⁶ · Sergio Tufik¹ · Jivaldo do Rosário Matos⁷ · Lucildes Pita Mercuri²

Received: 5 August 2016 / Accepted: 22 November 2016 / Published online: 2 January 2017
© Akadémiai Kiadó, Budapest, Hungary 2016

Abstract Ordered mesoporous silica, SBA-15, presents non-toxic nature; high pore volume and high surface area; thermal, hydrothermal and mechanical stabilities. These features may enable its use as a carrier for commonly prescribed drugs in psychiatric practice: citalopram (CIT) and risperidone (RIS). Thermogravimetry/derivative thermogravimetry (TG/DTG) and ultraviolet and visible absorption spectrophotometry (UV–Vis) were used to determine drug quantity into/onto ECIT (CIT encapsulated into SBA-15), ERIS (RIS encapsulated into SBA-15), MCIT (mixture of CIT with SBA-15) and MRIS (mixture of RIS with SBA-15). All materials were characterized

through: TG/DTG, differential scanning calorimetry, elemental analysis, Fourier transform infrared absorption spectrophotometry and nitrogen adsorption–desorption. A general solvent-based method for loading these psychoactive drugs into non-functionalized SBA-15 showed to retard their liberation in simulated gastric and intestinal media when compared to physical mixtures performance. It is expected that the functionalization of this nanostructured silica may increasingly extend the dissolution of CIT and RIS after encapsulation process, leading to application in controlled release systems.

Keywords Drug delivery · Ordered mesoporous silica · Controlled release · Solvent-based loading

✉ Lucildes Pita Mercuri
lpmercuri@gmail.com

¹ Departamento de Psicobiologia, Universidade Federal de São Paulo/Escola Paulista de Medicina, São Paulo 04023-062, Brazil

² Departamento de Ciências Exatas e da Terra, Instituto de Ciências Ambientais, Químicas e Farmacêuticas, Universidade Federal de São Paulo, Diadema, São Paulo 09913-030, Brazil

³ Faculdade de Ciências Farmacêuticas, Universidade de São Paulo, São Paulo 05513-970, Brazil

⁴ Departamento de Engenharia, Instituto Superior de Educação Santa Cecília, Universidade Santa Cecília, São Paulo 11045-907, Brazil

⁵ Centro de Ciência e Tecnologia de Materiais, Instituto de Pesquisas Energéticas e Nucleares, São Paulo 05508-900, Brazil

⁶ Departamento de Medicina, Universidade Federal de São Carlos, São Carlos, São Paulo 04023-061, Brazil

⁷ Laboratório de Análise Térmica Prof. Dr. Ivo Giolito, Instituto de Química, Universidade de São Paulo, São Paulo 05513-970, Brazil

Introduction

Ordered mesoporous silicas have been of great interest since their discovery in the 1990s [1]. Some of their applications include catalysis, fixation of biologically active species, separations and advanced optical [2]. SBA-15 silica belongs to this large family of materials, presenting high pore volume (up to $2.2 \text{ cm}^3 \text{ g}^{-1}$), high surface area (up to $1500 \text{ m}^2 \text{ g}^{-1}$) and thermal, hydrothermal and mechanical stabilities [3–5].

SBA-15 silica concentrations varying from 200 to $1000 \mu\text{g mL}^{-1}$ did not alter cell integrity of macrophages maintained in vitro [6]. Additionally, no differences related to mass and morphological parameters were observed in animal models followed up for 1 year after administration of this nanostructured silica [6]. Furthermore, SBA-15 was successfully tested in immunological practice as an effective adjuvant [7].

Since silica-based drug delivery platforms in controlled release have been extensively studied [8–11], it was opportune to apply this technology using different substances. Citalopram, one of the first selective serotonin reuptake inhibitors (SSRI) introduced in the market, has the main clinical use in the treatment of depression [12], and risperidone is one of the most widely prescribed antipsychotic medications, used for both acute and long-term maintenance in schizophrenia [13]. Moreover, these drugs had already been studied in controlled release but not using nanostructured silicas [14–16]. Therefore, it is providential to study the dissolution profile of these psychoactive agents from SBA-15 silica matrices because of the many benefits for patients by taking an oral controlled release formulation [17, 18], including maintenance of optimum drug concentration, increased duration of therapeutic effect, improved efficiency of treatment with less amount of drug, minimized side effects, less frequent administration and increased patient convenience and compliance [18].

This study aimed to provide a starting point for evaluating the *in vitro* release of citalopram and risperidone encapsulated into non-functionalized SBA-15 in comparison with the performance of physical mixtures.

Materials and methods

Synthesis of ordered mesoporous silica, SBA-15

SBA-15 was synthesized under acid conditions by self-assembly with triblock copolymer template $\text{EO}_{20}\text{PO}_{70}\text{EO}_{20}$ [poly(ethylene oxide)-poly(propylene oxide)-poly(ethylene oxide)] (Pluronic P123, BASF, Germany) and tetraethoxysilane (TEOS 98%, Sigma-Aldrich, USA) as described elsewhere [4].

Encapsulation and physical mixing

To encapsulate citalopram hydrobromide ($\text{C}_{20}\text{H}_{22}\text{BrFN}_2\text{O}$, LIBBS, Brazil) and risperidone ($\text{C}_{23}\text{H}_{27}\text{FN}_4\text{O}_4$, Biosintética, Brazil) into SBA-15, samples of silica were added to citalopram-ethanol and risperidone-methanol solutions (ca. 1.7 mg of drug per milliliter of solvent) in proportion 1:1 (SBA-15: drug) and stirred for 6 and 24 h, respectively. These solutions were decanted, and the supernatants were withdrawn. Remaining materials, named risperidone encapsulated into SBA-15 (ERIS) and citalopram encapsulated into SBA-15 (ECIT), were dried in a stove at 70 °C for solvents vaporization. Physical mixtures, MCIT and MRIS, were obtained blending SBA-15 (ca. 91.6%) with citalopram hydrobromide (ca. 8.4%) and SBA-15 (ca. 93.8%) with risperidone (ca. 6.2%), respectively, by

geometrical dilution using mortar and pestle. The blends were gently ground for at least 10 min to assure homogenization.

Characterization of the materials

Thermogravimetry (TG) and derivative thermogravimetry (DTG)

Thermogravimetric evaluations were performed on a TGA-51 thermobalance (Shimadzu, Japan) under dynamic air atmosphere (50 mL min^{-1}), using platinum pan, at a heating rate (V_H) of $10 \text{ }^\circ\text{C min}^{-1}$ and sample mass ranging from 10 to 25 mg.

Differential scanning calorimetry (DSC)

Assays were carried out using a DSC-50 cell (Shimadzu, Japan) with sample mass between 1.70 and 1.75 mg under dynamic nitrogen atmosphere (100 mL min^{-1}), using sealed aluminum pans, at a heating rate (V_H) of $10 \text{ }^\circ\text{C min}^{-1}$.

Nitrogen adsorption-desorption

The N_2 adsorption-desorption isotherms were obtained at $-196 \text{ }^\circ\text{C}$ under continuous adsorption conditions, utilizing an ASAP 2010 volumetric sorption analyzer (Micromeritics, USA). The Brunauer-Emmett-Teller (BET) method was utilized to calculate the surface area, and the Barrett-Joyner-Halenda (BJH) method was used to calculate pore size and volume.

Elemental analysis (EA)

Carbon, nitrogen and hydrogen percentages in the samples were obtained through a CHN 2400 elemental analyzer (Perkin-Elmer, USA).

Fourier transform infrared absorption spectrophotometry (FT-IR)

FT-IR spectra were recorded in KBr dispersion using an MB 102 FT-IR spectrophotometer (Bomem, USA) at room temperature in the $400\text{--}4000 \text{ cm}^{-1}$ range.

In vitro studies

Dissolution tests were carried out utilizing 500 mL of media kept at $37 \pm 0.5 \text{ }^\circ\text{C}$. These experiments were conducted in a VK 7025 dissolution tester (Varian, USA). The drugs were added to mixing vats using United States Pharmacopeia (USP) Apparatus I, i.e., baskets, and the

homogenization was assured at a stirring speed of 50 rpm, under the form of either an encapsulated formulation or as a physical mixture [19]. Simulated gastric fluid (SGF, 0.1 M HCl, pH = 1.2) and simulated intestinal fluid (SIF, phosphate buffer, pH = 6.8) were prepared based on USP XXXI (2008) [20]. SGF and SIF were deaerated by sonication in a USC 1450 ultrasonic bath (Unique, Brazil) for 10 min. Samples of 7 mL were manually withdrawn between 5 and 90, 5 and 120 or 10 and 120 min from media and filtered over 0.20 μm (Sartorius, Germany) or 0.45 μm (AxyGen Scientific, USA) membrane filters.

Ultraviolet and visible absorption spectrophotometry (UV-Vis)

The quantification of CIT and RIS in all aliquots from dissolution experiments was performed by a U-2910 UV-Vis spectrophotometer (Hitachi, Japan). Either the maximum wavelengths (λ_{max}) used for absorbance measurements of CIT and RIS (239 and 280 nm, respectively) or the standard methods assumed in this section were based on previously validated procedures [19, 21].

Results and discussion

CIT and RIS were thermally stable until 250 and 240 $^{\circ}\text{C}$, respectively, as shown in TG/DTG curves (Figs. 1, 2). The thermal decomposition of the drugs was initiated above these temperatures. MCIT contained around 8.7% of CIT and MRIS contained *circa* 7.0% of RIS. These contents were estimated by ultraviolet and visible absorption spectrophotometry (UV-Vis). Values of approximately 8.4% of CIT encapsulated into SBA-15 and 6.1% of RIS encapsulated into SBA-15 were determined by TG/DTG, considering the mass loss between 200 and 900 $^{\circ}\text{C}$. TG/DTG was also adopted for drug quantification as CIT and RIS were

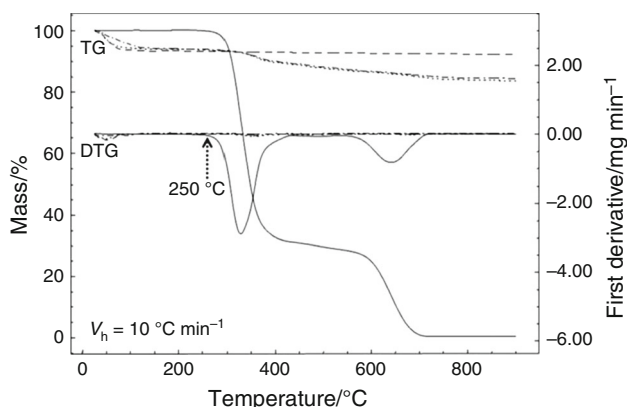


Fig. 1 TG/DTG curves: SBA-15 (line with space), CIT (line) MCIT (small line with space) and ECIT (line with small line)

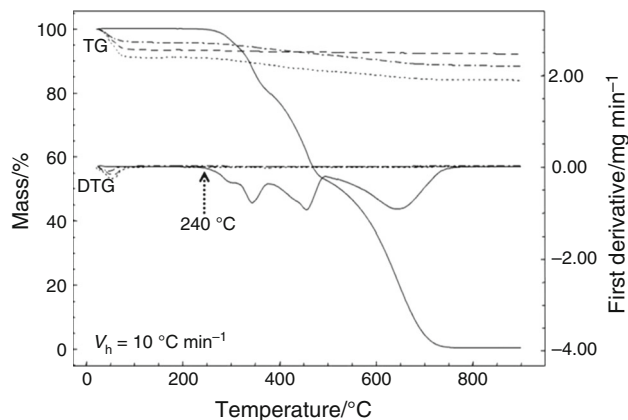


Fig. 2 TG/DTG curves: SBA-15 (line with space), RIS (line), MRIS (small line with space) and ERIS (line with small line)

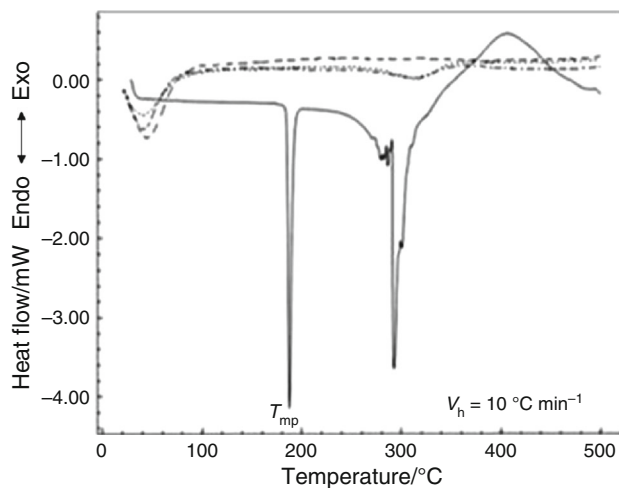


Fig. 3 DSC curves: SBA-15 (line with space), CIT (line), MCIT (small line with space) and ECIT (line with small line)

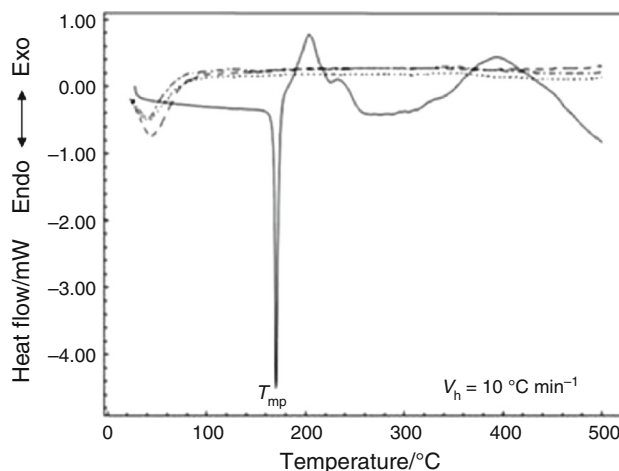


Fig. 4 DSC curves: SBA-15 (line with space), RIS (line), MRIS (small line with space) and ERIS (line with small line)

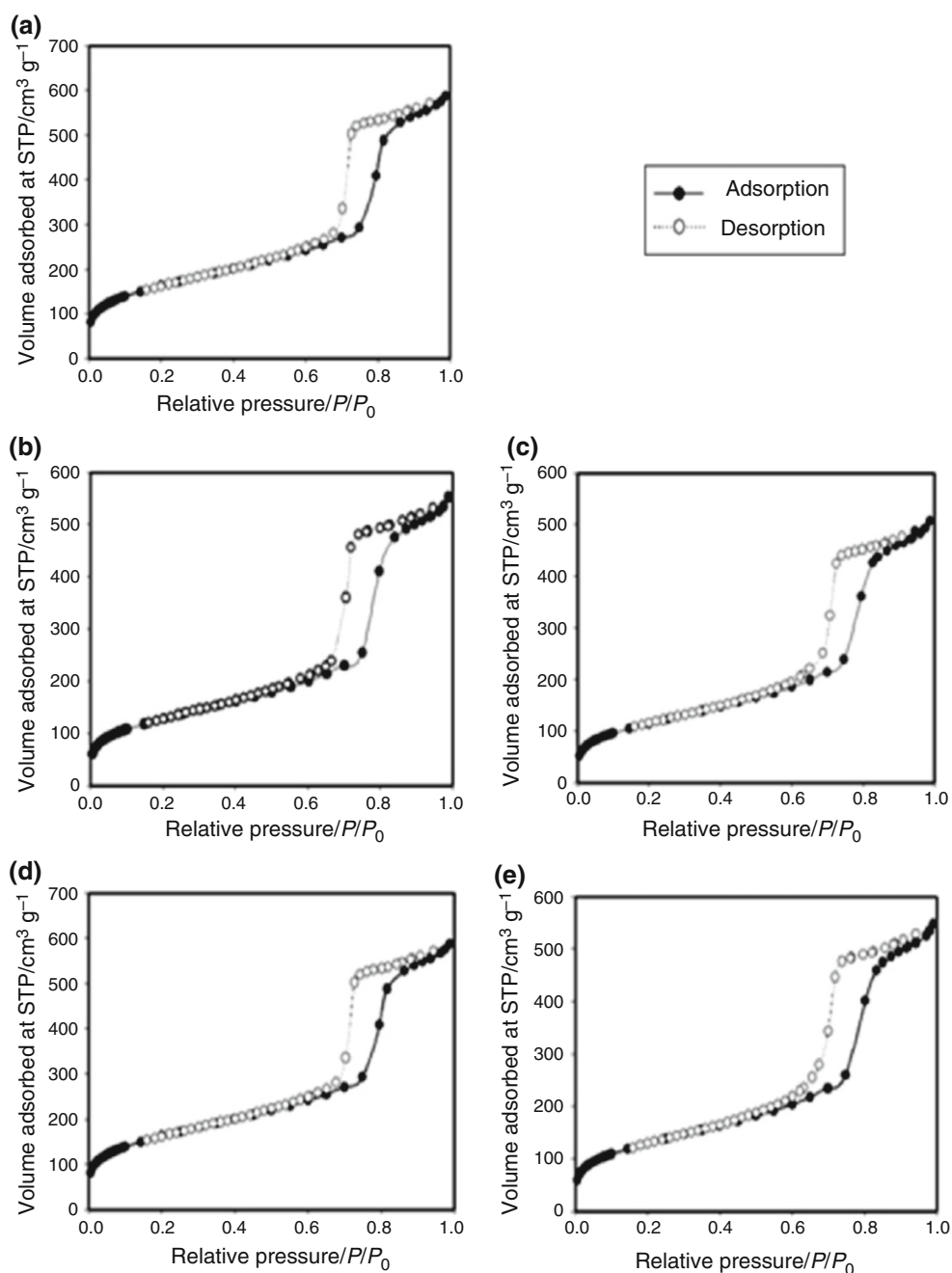
not supposed to be completely released from the mesopores of SBA-15 in aqueous hydrochloric acid solution for UV–Vis measurements.

CIT showed a melting point at 188 °C and RIS melted at 170 °C as shown in DSC curves (Figs. 3, 4). No melting peak was observed in DSC curves of ECIT, MCIT, ERIS and MRIS samples, neither at the bulk melting point, nor at depressed temperatures. It was hypothesized that the adsorbed drugs (CIT and RIS) fractions were found to be noncrystalline [3]. The absence of melting peaks reflects

the noncrystalline state of the confined molecules, and the absence of bulk melting in physical mixtures reflects a strong interaction with the silica surface induced by simple physical blending [3].

Figure 5 shows the N₂ adsorption–desorption isotherms. All isotherms were of type IV according to the IUPAC classification and showed H1 hysteresis loop which is dominant in ordered mesoporous materials with uniform cylindrical pores [22]. The Brunauer–Emmett–Teller (BET) method was used to evaluate the specific surface

Fig. 5 N₂ adsorption–desorption isotherms: SBA-15 (a), ECIT (b), MCIT (c), ERIS (d) and MRIS (e)



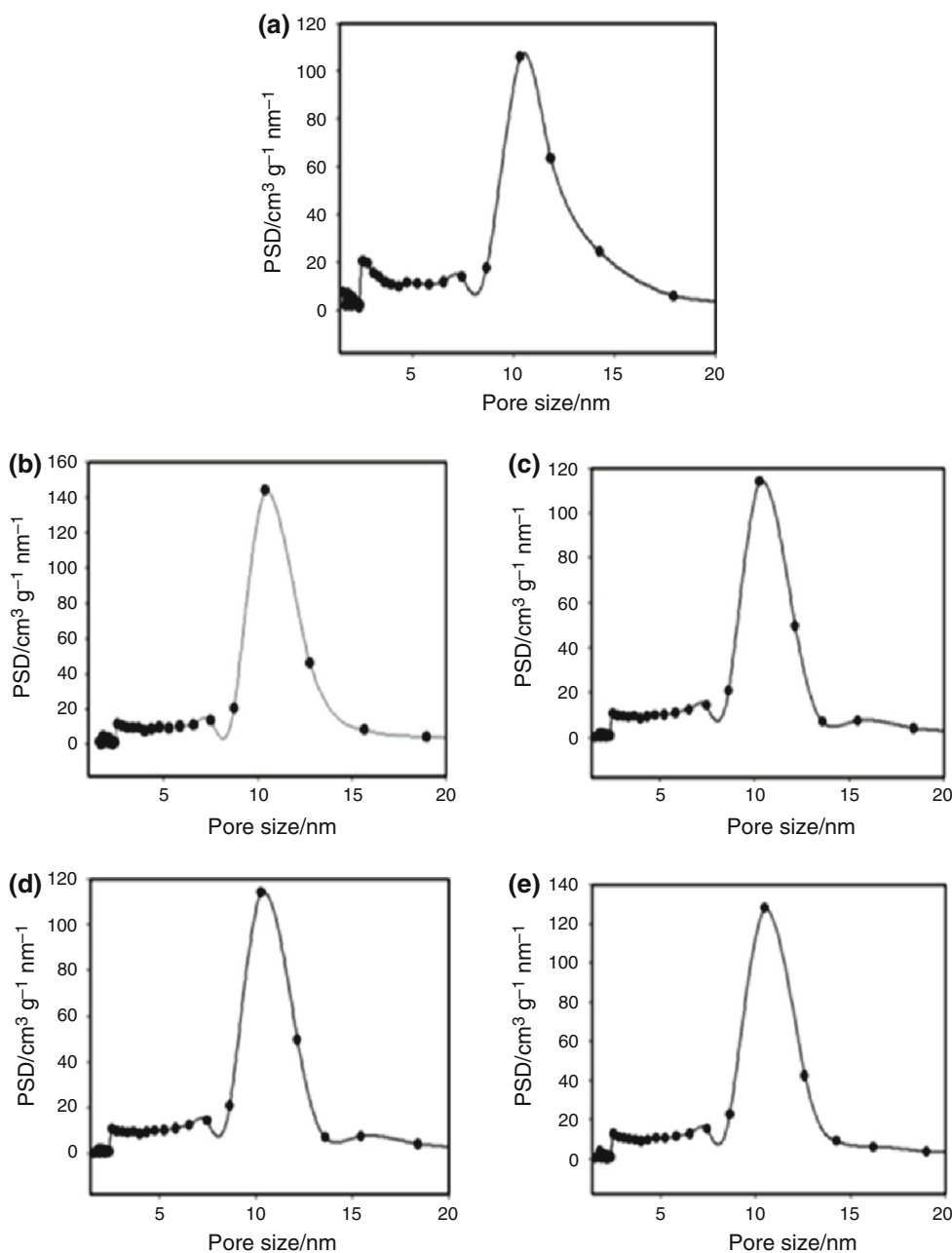
area (S_{BET}), and the Barrett–Joyner–Halenda (BJH) method was utilized to measure the pore diameter distribution. The textural parameters are shown in Table 1.

Table 1 Textural parameters according to N_2 adsorption–desorption

Sample	BET surface area/ $m^2 g^{-1}$ S_{BET}	BJH pore size/nm
SBA-15	566.2	6.5
ECIT	451.6	6.6
MCIT	410.2	6.5
EIS	492.3	6.4
MRIS	458.0	6.4

Although CIT and RIS have not occupied all the available space of SBA-15 preparations, N_2 adsorption–desorption data demonstrated that ECIT, MCIT, ERIS and MRIS had reduction in surface area. The decreased values of S_{BET} of ECIT, MCIT, ERIS and MRIS samples, compared with pure SBA-15, may have an explanation in the fact that drug molecules occupied these spaces [23]. It is conceivable that the internal and external surface of the cylindrical pores was partially covered with the drug molecules [23]. The pore size remained practically unchanged, and predominant diameter was 10 nm, according to the pore size distribution (PSD) results (Fig. 6).

Fig. 6 Pore size distribution (PSD) obtained from N_2 adsorption–desorption isotherms at $-196\text{ }^\circ\text{C}$: SBA-15 (a), ECIT (b), MCIT (c), ERIS (d) and MRIS (e)



Elemental analysis (EA) results (Table 2) confirmed that CIT and RIS were present in the SBA-15 formulations by remarkable increases of carbon, nitrogen and hydrogen levels in comparison with pure silica.

The FT-IR spectrum of SBA-15 showed an intense band at 1089 cm^{-1} assigned to silanol groups (Si-OH) that was observed in the other spectra of silica-drug materials between 1081 and 1086 cm^{-1} ; CIT spectrum presented an

Table 2 Elemental analysis results

Sample	C/%	H/%	N/%
SBA-15	0.41	0.68	0.14
CIT	59.37	5.90	7.06
RIS	67.23	6.30	13.47
ECIT	7.00	1.49	0.45
MCIT	5.77	1.27	0.85
ERIS	5.25	1.74	0.80
MRIS	4.52	1.55	0.88

absorption band at 2229 cm^{-1} , corresponding to the stretching of $\text{C}\equiv\text{N}$ group, also observed in the MCIT and ECIT spectra between 2234 and 2235 cm^{-1} , respectively; the spectrum of RIS showed a band at 1650 cm^{-1} assigned to the stretching of $\text{C}=\text{C}$ aromatic ring, likewise observed in the spectra of MRIS and ERIS between 1637 and 1635 cm^{-1} , respectively. These observations gave support to confirm the presence of CIT in the samples of ECIT and MCIT, as well as the presence of RIS in the ERIS and MRIS samples. No interactions were found using FT-IR for all materials (Fig. 7).

Dissolution profiles demonstrated that drug unloading from ECIT and ERIS was slower than from the physical mixtures MCIT and MRIS in simulated gastrointestinal medium [Fig. 8–11 (measures are expressed in mean values, $n = 2$)].

Dissolution in SGF: The release of CIT from ECIT reached 83.1% (SD = 0.1%) after 120 min and 90.1% (SD = 10.2%) from MCIT after 10 min (Fig. 8); the liberation of RIS from ERIS reached 80.7% (SD = 0.3%)

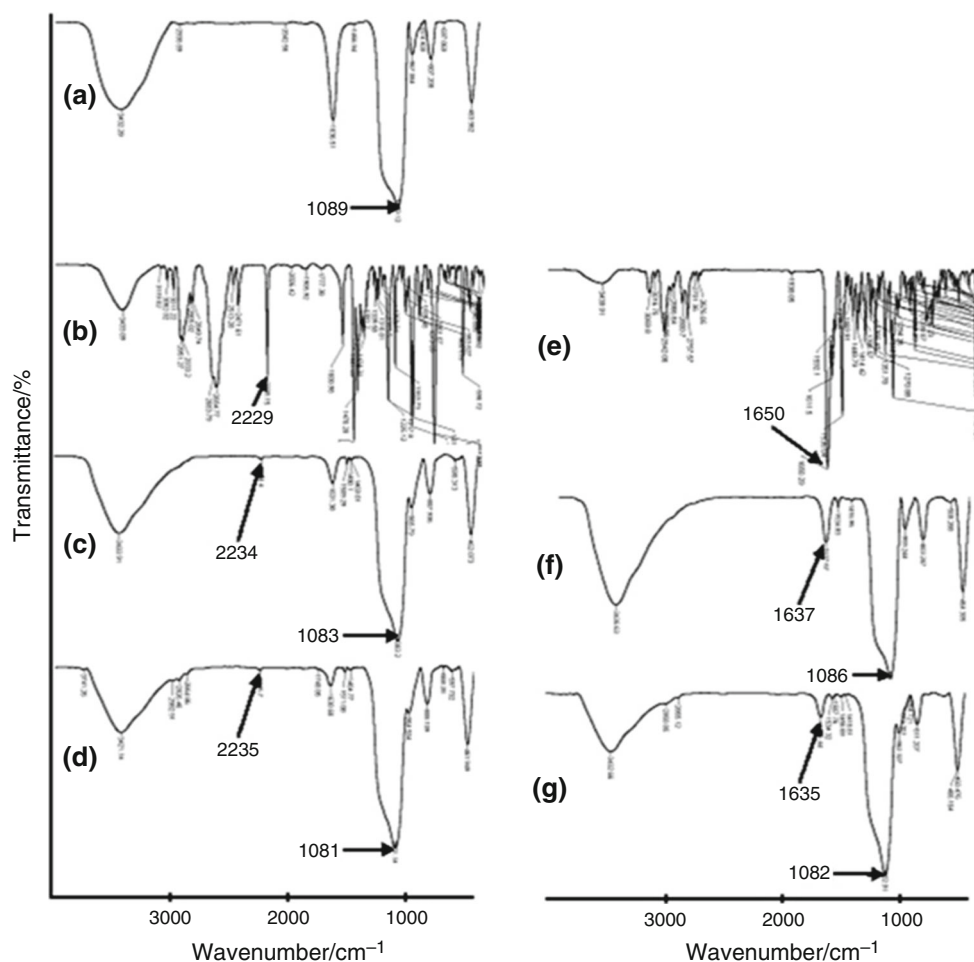


Fig. 7 FT-IR spectra: SBA-15 (a), CIT (b), MCIT (c), ECIT (d), RIS (e), MRIS (f) and ERIS (g)

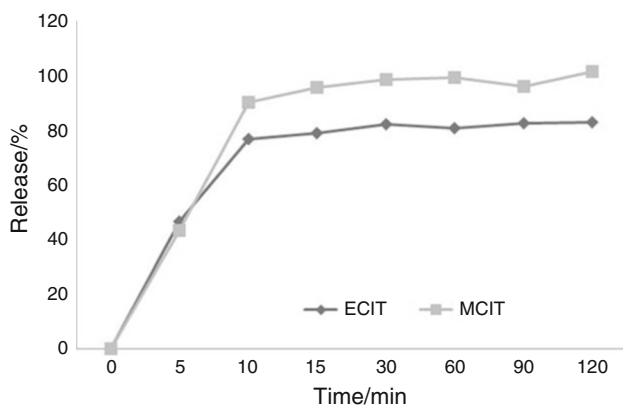


Fig. 8 In vitro profiles: ECIT (line with diamond) and MCIT (line with square) in simulated gastric fluid, pH = 1.2. *ECIT 90 min, $n = 1$ (one of the samplings was not concluded due to technical issues)

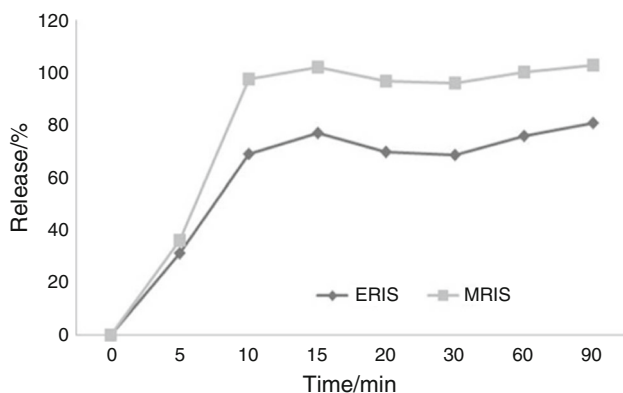


Fig. 9 In vitro profiles: ERIS (line with diamond) and MRIS (line with square) in simulated gastric fluid, pH = 1.2

after 90 min, while MRIS released 97.6% (SD = 2.8%) of RIS after 10 min (Fig. 9).

Dissolution in SIF: The CIT unloading from ECIT reached 69.1% (SD = 0.8%) after 120 min and 90.8% (SD = 3.1%) from MCIT as shown in Fig. 10; ERIS released 31.1% (SD = 1.9%) of RIS after 120 min, whereas MRIS released 68.2% (SD = 9.0%) of RIS in the same period of time (Fig. 11).

It was possible to observe oscillations in the dissolution profiles (Figs. 8–11), in which determined drug liberation rates were followed by inferior drug releases. These types of variation have been found in the literature [24–26], and they may be a subject of further investigation. Besides, an increase in the sample size is necessary for more accurate results.

The SGF was more favorable to drug release probably due to the fact that the synthesis of SBA-15 silica had been carried out in acid medium. Moreover, the lower dissolution rates of RIS may be explained by its low solubility:

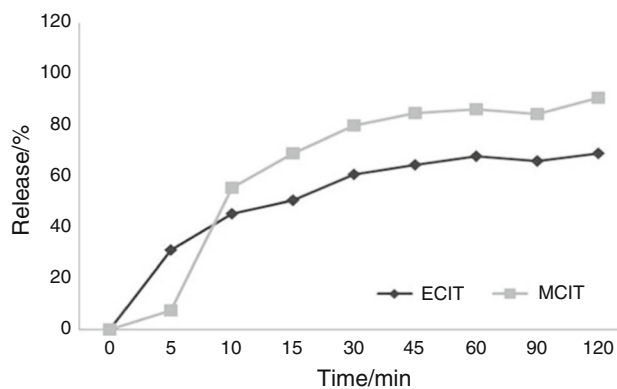


Fig. 10 In vitro profiles: ECIT (line with diamond) and MCIT (line with square) in simulated intestinal fluid, pH = 6.8

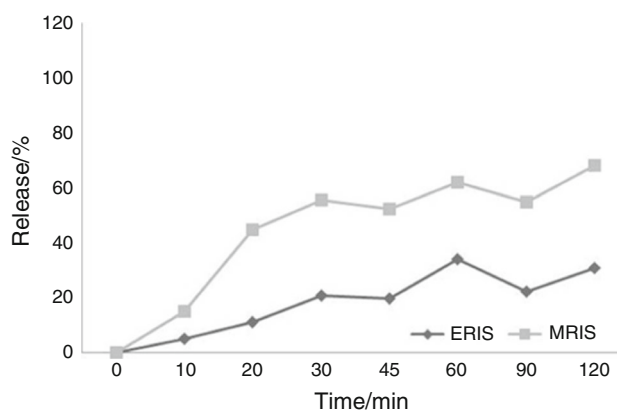


Fig. 11 In vitro profiles: ERIS (line with diamond) and MRIS (line with square) in simulated intestinal fluid, pH = 6.8

RIS is labeled as class II compound according to the Biopharmaceutics Classification System (BCS); otherwise, CIT possesses high solubility, BCS class I drug. In addition, a relatively simple solvent-based method for loading psychoactive drugs into non-functionalized SBA-15 decreased the liberation of the drugs from ECIT and ERIS in simulated gastrointestinal medium in comparison with physical mixtures profiles. The faster drug release from physical blendings may be explained in terms of the localization of the drugs fraction: Internally deposited drug molecules need time to diffuse out the pores [3].

Conclusions

A general solvent-based method utilized for encapsulation of citalopram and risperidone into SBA-15 silica was able to retard the drugs liberation. By the way, these findings demonstrated that the incorporation of functional groups on the surface of SBA-15 silica is necessary for better control over loading and release [27]. Functionalized mesoporous

silica offers promising possibilities for drug delivery as reported elsewhere [27–29]. Accordingly, there are perspectives to optimize the encapsulation process using functionalized mesoporous silicas (this step includes an increase of the sample size and an extension of the dissolution tests to observe the complete drug unloading) and also to investigate the therapeutic efficacy of the encapsulated drugs. We expect to apply ordered mesoporous silica SBA-15 in controlled release formulations to improve patients' compliance throughout citalopram and risperidone treatments.

Acknowledgements We would like to thank the Coordenação de Aperfeiçoamento de Pessoal de Nível Superior (CAPES) and the Associação Fundo de Incentivo à Psicofarmacologia (AFIP).

References

- Kresge CT, Leonowics ME, Roth WJ, Vartuli JC, Beck JS. Ordered mesoporous molecular sieves synthesized by a liquid-crystal template mechanism. *Nature*. 1992;359:710–2.
- Stein A, Melde BJ, Schroden RC. Hybrid inorganic-organic mesoporous silicates-nanoscope reactors coming of age. *Adv Mater*. 2000;12:1403–19.
- Van Speybroeck M, Barillaro V, Thi TD, Mellaerts R, Martens J, Humbeeck JV, Vermant J, Annaert P, Mooter GVD, Augustijns PJ. Ordered mesoporous silica material SBA-15: a broad-spectrum formulation platform for poorly soluble drugs. *J Pharm Sci*. 2009;98:2648–58.
- Matos JR, Mercuri LP, Kruk M, Jaroniec M. Toward the synthesis of extra-large-pore MCM-41 analogues. *Chem Mater*. 2001;13:1726–31.
- Cassiers K, Linssen T, Mathieu M, Benjelloun M, Schrijnemakers K, Van der Voort P, Cool P, Vansant EF. A detailed study of thermal, hydrothermal, and mechanical stabilities of a wide range of surfactant assembled mesoporous silicas. *Chem Mater*. 2002;14:2317–24.
- Carvalho LV, Ruiz RDC, Scaramuzzi K, Marengo EB, Matos JR, Tambourgi DV, Fantini MCA, Sant'Anna OA. Immunological parameters related to the adjuvant effect of the ordered mesoporous silica SBA-15. *Vaccine*. 2010;28:7829–36.
- Mercuri LP, Carvalho L, Lima F, Quayle C, Fantini M, Tanaka G, Cabrera W, Furtado M, Tambourgi D, Matos JR, Sant'Anna OA. Ordered mesoporous silica SBA-15: a new effective adjuvant to induce antibody response. *Small*. 2006;2:254–6.
- Ehlert N, Badar M, Christel A, Lohmeier SJ, Luessenhop T, Stieve M, Lenarz T, Mueller PP, Behrens P. Mesoporous silica coatings for controlled release of the antibiotic ciprofloxacin from implants. *J Mater Chem*. 2011;21:752–60.
- Ni M, Xu QQ, Yin JZ. Preparation of controlled release nanodrug ibuprofen supported on mesoporous silica using supercritical carbon dioxide. *J Mater Res*. 2012;27:2902–10.
- Chowdhury MA. The Controlled release of drugs and bioactive compounds from mesoporous silica nanoparticles. *Curr Drug Deliv*. 2016;13:839–56.
- Karimi M, Mirshekari H, Aliakbari M, Sahandi-Zangabad P, Hamblin MR. Smart mesoporous silica nanoparticles for controlled-release drug delivery. *Nanotechnol Rev*. 2016;5:195–207.
- Pires SA, Mussel WN, Yoshida MI. Solid-state characterization and pharmaceutical compatibility between citalopram and excipients using thermal and non-thermal techniques. *J Therm Anal Calorim*. 2016;. doi:10.1007/s10973-016-5769-z.
- Madaan V, Bestha DP, Kolli V, Jauhari S, Burket RC. Clinical utility of the risperidone formulations in the management of schizophrenia. *Neuropsychiatr Dis Treat*. 2011;7:611–20.
- Abdouss M, Asadi E, Azodi-Deilami S, Beik-mohammadi N, Aslanzadeh SA. Development and characterization of molecularly imprinted polymers for controlled release of citalopram. *J Mater Sci Mater Med*. 2011;22:2273–81.
- Badshah A, Subhan F, Rauf K, Bukhari NI, Shah K, Khan S, Ahmed Z, Khan I. Development of controlled-release matrix tablet of risperidone: influence of Methocel®- and Ethocel®-based novel polymeric blend on in vitro drug release and bioavailability. *AAPS PharmSciTech*. 2011;12:525–33.
- Siafaka PI, Barmapalexis P, Lazaridou M, Papageorgiou GZ, Koutris E, Karavas E, Kostoglou M, Bikiaris DN. Controlled release formulations of risperidone antipsychotic drug in novel aliphatic polyester carriers: data analysis and modelling. *Eur J Pharm Biopharm*. 2015;94:473–84.
- Nokhodchi A, Raja S, Patel P, Asare-Addo K. The role of oral controlled release matrix tablets in drug delivery systems. *Bioimpacts*. 2012;2:175–87.
- Wen H, Park K, editors. Oral controlled release formulation design and drug delivery: theory to practice. New Jersey: Wiley; 2010. p. 1.
- Menegola J, Steppe M, Schapoval EE. Dissolution test for citalopram in tablets and comparison of in vitro dissolution profiles. *Eur J Pharm Biopharm*. 2007;67:524–30.
- USP 31: United States Pharmacopeial Convention. The United States pharmacopeia: the national formulary (USP XXXI-NF26). Rockville: The United States Pharmacopeial Convention, 2008, p. 813–4.
- Kumar MS, Smith AA, Vasagam GA, Muthu AK, Manavalan R. Development of analytical method for risperidone by UV spectrophotometry. *Inter J Pharma Sci Res*. 2010;1:122–6.
- García-Martínez J, Li K, editors. Mesoporous zeolites: preparation, characterization and applications. Weinheim: Wiley; 2015. p. 358.
- Lopez T, Ortiz-Islas E, Lopez M, Flores J, Corona T. Occlusion of Interferon® and Copaxone® on SBA-15 silica reservoirs for their use in the treatment of demyelization diseases. *J Nanomater Mol Nanotechnol*. 2013;2:1–6.
- Barrêto Gomes AP, Souza FS, Macêdo RO. Thermal and dissolution kinetics of ampicillin drug and capsules. *J Therm Anal Calorim*. 2003;72:545–8.
- Patel PV, Patel H, Panchal SS, Mehta T. Self micro-emulsifying drug delivery system of tacrolimus: formulation, in vitro evaluation and stability studies. *Int J Pharm Investig*. 2013;3:95–104.
- Ha ES, Baek I, Yoo JW, Jung Y, Kim MS. Improving dissolution and oral bioavailability of pranlukast hemihydrate by particle surface modification with surfactants and homogenization. *Drug Des Devel Ther*. 2015;9:3257–66.
- Bouchoucha M, Côté MF, Gaudreault RC, Fortin MA, Kleitz F. Size-controlled functionalized mesoporous silica nanoparticles for tunable drug release and enhanced anti-tumoral activity. *Chem Mater*. 2016;28:4243–58.
- Brühwiler D. Postsynthetic functionalization of mesoporous silica. *Nanoscale*. 2010;2:887–92.
- Yang P, Gai S, Lin J. Functionalized mesoporous silica materials for controlled drug delivery. *Chem Soc Rev*. 2012;41:3679–98.